

# Elucidating the biosynthesis of 2-carboxyarabinitol 1-phosphate through reduced expression of chloroplastic fructose 1,6-bisphosphate phosphatase and radiotracer studies with $^{14}\text{CO}_2$

P. John Andralojc<sup>\*†</sup>, Alfred J. Keys<sup>\*</sup>, Jens Kossmann<sup>‡</sup>, and Martin A. J. Parry<sup>\*</sup>

<sup>\*</sup>IACR-Rothamsted, Crop Performance & Improvement Division, West Common, Harpenden, Hertfordshire AL5 2JQ, United Kingdom; and <sup>†</sup>Risø National Laboratory, Plant Research Department, Building PBK-776, P.O. Box 49, Frederiksborgvej 399, DK-4000 Roskilde, Denmark

Edited by Bob B. Buchanan, University of California, Berkeley, CA, and approved February 5, 2002 (received for review March 21, 2001)

**2-Carboxyarabinitol 1-phosphate limits photosynthetic  $\text{CO}_2$  assimilation at low light because it is a potent, naturally occurring inhibitor of ribulose 1,5-bisphosphate carboxylase/oxygenase. Evidence is presented that this inhibitor is derived from chloroplastic fructose 1,6-bisphosphate. First, transgenic plants containing decreased amounts of chloroplastic fructose 1,6-bisphosphate phosphatase contained increased amounts of fructose 1,6-bisphosphate and 2-carboxyarabinitol 1-phosphate and greatly increased amounts of the putative intermediates hamamelose and 2-carboxyarabinitol, which in some cases were as abundant as sucrose. Second, French bean leaves in the light were shown to incorporate  $^{14}\text{C}$  from  $^{14}\text{CO}_2$  sequentially into fructose 1,6-bisphosphate, hamamelose biphosphate, hamamelose monophosphate, hamamelose, and 2-carboxyarabinitol. As shown previously,  $^{14}\text{C}$  assimilated by photosynthesis was also incorporated into 2-carboxyarabinitol 1-phosphate during subsequent darkness.**

**R**ibulose 1,5-bisphosphate carboxylase/oxygenase (Rubisco; EC 4.1.1.39) is responsible for the assimilation of  $\text{CO}_2$  during photosynthesis in higher plants, algae, and many photosynthetic bacteria. In higher plants this enzyme is regulated by changes in pH, by the concentration of  $\text{Mg}^{2+}$  and  $\text{CO}_2$ , and by other stromal activators and inhibitors, in conjunction with the light-dependent enzyme, Rubisco activase (reviewed in ref. 1). Rubisco is only active when an essential lysine residue within the large subunit is carbamylated with  $\text{CO}_2$  followed by coordination of  $\text{Mg}^{2+}$  to form a ternary complex at the catalytic site (2). 2-Carboxy-D-arabinitol 1-phosphate (CA1P) is a naturally occurring analogue of the transition-state of the carboxylase reaction, which binds tightly to the active site of carbamylated Rubisco and thus inhibits catalytic activity (3, 4). CA1P is important in the diurnal regulation of photosynthesis, particularly during periods of low irradiance or darkness (5, 6). On transition from dark to light, Rubisco activase promotes the release of CA1P from the catalytic site of Rubisco (7), and free CA1P is rendered noninhibitory by the action of a light-activated CA1P-phosphatase (8–10). *In vitro*, CA1P bound to the active site of Rubisco can be released by treatment with sulfate ions and Rubisco subsequently separated from CA1P by gel filtration or polyethylene glycol precipitation, to restore the activity of the enzyme (11, 12). Recent work indicates an additional role for CA1P in the protection of Rubisco from degradation by stromal proteases (12). Therefore, CA1P may influence the turnover, as well as the activity, of this enzyme.

The investigation of CA1P biosynthesis from recently assimilated carbon has benefited from the recognition of the structural similarity between the branch-chain sugar phosphate, hamamelose 2',5-bisphosphate (HBP), and CA1P (13). Good evidence exists for the passage of assimilated  $\text{CO}_2$  to HBP and

thence hamamelose (2-hydroxymethyl-D-ribose) by way of the Calvin cycle intermediate FBP. First, the pool of HBP is saturated with  $^{14}\text{C}$  from  $^{14}\text{CO}_2$  as rapidly as the pools of Calvin cycle intermediates sedoheptulose 1,7-bisphosphate and sedoheptulose 7-phosphate, whereas hamamelose monophosphate (HMP) and free hamamelose continued to accumulate further  $^{14}\text{C}$  during the same period. These observations suggested the proximity of HBP synthesis to the Calvin cycle and that HBP was kinetically competent to be a precursor of HMP and hamamelose (14). Second, FBP was converted into HBP in the presence of isolated spinach chloroplasts, suggesting a precursor-product relationship between FBP and HBP (14). The passage of  $^{14}\text{C}$  from  $^{14}\text{CO}_2$  into HBP by isolated chloroplasts has also been reported (15). The conversion of  $^{14}\text{C}$ -labeled hamamelose into carboxyarabinitol in the light and into carboxyarabinitol and CA1P in the dark (no other radiolabeled products were detected) has been demonstrated (16). Furthermore, the flow of carbon from hamamelose to CA1P could be completely prevented by prior leaf infiltration with DTT, whereas that from hamamelose to CA still persisted, implying that the conversion of hamamelose to CA does not require prior synthesis of CA1P (16). This persistence, in combination with the demonstration that CA gives rise exclusively to CA1P in darkened leaves (16, 17), provides strong evidence for the biosynthetic pathway shown (Fig. 1).

To test this putative pathway, potato plants expressing the gene for chloroplastic fructose 1,6-bisphosphate phosphatase (FBPase) in the antisense orientation were examined. These plants have lower FBPase activities and contain more FBP than their wild-type counterparts (18). Because FBP marks the entry point of recently assimilated carbon into the proposed pathway, the present demonstration that such plants contain more hamamelose, CA, and CA1P provides further support for this biosynthetic route (Fig. 1). This sequence was further endorsed by observing the passage of  $^{14}\text{C}$  from assimilated  $^{14}\text{CO}_2$  through the proposed intermediates during steady-state photosynthesis.

## Materials and Methods

**Plants and Leaf Sampling.** Potato plants (*Solanum tuberosum* L.), with or without the chloroplast FBPase gene in the antisense

This paper was submitted directly (Track II) to the PNAS office.

Abbreviations: Rubisco, ribulose-1,5-bisphosphate carboxylase/oxygenase; hamamelose, 2-hydroxymethyl-D-ribose; CA1P, 2-carboxy-D-arabinitol 1-phosphate; CA, 2-carboxy-D-arabinitol; H, hamamelose; HMP, hamamelose monophosphate; HBP, hamamelose 2',5-bisphosphate; F, fructose; FBP, fructose 1,6-bisphosphate; FBPase, FBP phosphatase.

<sup>†</sup>To whom reprint requests should be addressed. E-mail: john.andralojc@bbsrc.ac.uk.

The publication costs of this article were defrayed in part by page charge payment. This article must therefore be hereby marked "advertisement" in accordance with 18 U.S.C. §1734 solely to indicate this fact.

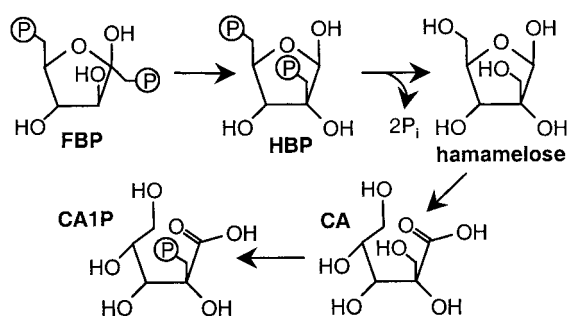


**Fig. 1.** Proposed pathway for CA1P biosynthesis from Calvin cycle intermediate, FBP.

orientation (18), were grown under glass (14 h at 20°C during the day, 10 h at 16°C during the night) with supplemental lighting to ensure a minimum daylight irradiance (photosynthetic photon flux) of 300  $\mu\text{mol photons m}^{-2}\text{s}^{-1}$ . The youngest fully expanded leaves were sampled in the middle of the photoperiod or 1 h before dawn, by rapidly freeze-clamping to the temperature of liquid nitrogen. Samples were stored in liquid nitrogen until assayed. Leaves of French bean (*Phaseolus vulgaris* L. cv. Tendergreen), grown as described above, were used in the pulse-chase experiments and for the quantitation of HMP and HBP in leaves, 12 days after sowing.

**Enzyme Assays.** The extraction and assay of Rubisco were as described (11). In brief, the initial activity (*i*) was the activity of Rubisco after rapid extraction into buffer, without further treatment. The total activity (*t*) was determined after preincubating an aliquot of the same extract in 10 mM NaHCO<sub>3</sub> and 20 mM MgCl<sub>2</sub> for 3 min at 25°C to activate vacant, noncarbamylated catalytic sites before adding substrate RuBP. The maximal activity (*m*) was determined after the sulfate-dependent displacement of tight binding inhibitors from the catalytic site, separation of Rubisco from low molecular weight solutes, followed by activation with NaHCO<sub>3</sub> and MgCl<sub>2</sub>, as above. FBP phosphatase activity was determined as described (18), ensuring prior activation of the enzyme by preincubation with 50 mM DL-DTT (Cleland's Reagent) for 10 min at 25°C.

**FBP, Hamamelose, CA, and CA1P Quantification.** Quantification of FBP, hamamelose, CA, and CA1P was determined by using a radioisotope-dilution procedure, based on the dilution of exogenous, radiolabeled metabolite by the nonradiolabeled equivalent from the extract (19). Leaf discs (10 per sample, each disk taken from distinct leaves of three separate plants, giving a total area of 25 or 50 cm<sup>2</sup>) were ground to a fine powder in liquid nitrogen together with 3 ml of 3.5% (vol/vol) trifluoroacetic acid/0.15% (wt/vol) 8-hydroxyquinoline. As the mixture began to thaw, <sup>14</sup>C-labeled FBP, hamamelose, CA, and/or CA1P were mixed in (15 nmol of each, of specific radioactivity 3 Ci mol<sup>-1</sup>; 1 Ci = 37 GBq). After 15 min at 0°C, the solution was clarified by centrifugation and lipophilic and cationic compounds removed by reverse-phase (C<sub>18</sub>) and Dowex-50 (H<sup>+</sup> form) chromatography, respectively, as described (20). The (Tris) neutralized mixture was divided into neutral (containing hamamelose), weakly anionic (CA), and strongly anionic (CA1P or FBP) fractions by using columns (25 mm × 7 mm) of Dowex-1 (formate form) by collecting the unbound, 0.2 and 0.5 M sodium formate washes (4 ml each), respectively. These compounds were subsequently purified by one or more rounds of HPLC as described below (DX500 chromatography system, with ED 40 electrochemical detector, Dionex). Final, quantitative, peak detection was by pulsed amperometry and by determination of the radioactivity of the purified sample. The amount of each

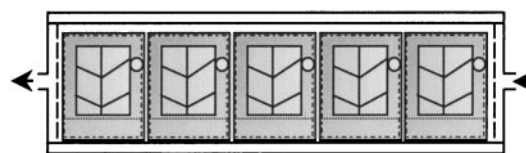


**Fig. 2.** Schematic diagram of chamber used for pulse-chase experiment. Leaf segments (light gray) in water-filled plastic troughs were contained entirely within the holders (dark gray), as indicated by broken and dotted lines, respectively. Magnets (open circles) were mounted on the side facing away from the light source. Arrows indicate gas flow.

component in the leaf sample was calculated from the ratio between the two measurements, relative to that of the radiolabeled standard (19). Hamamelose (21) and CA1P (22) were purified as reported. FBP was resolved by anion-exchange HPLC with a CarboPac PA1 column (4 × 250 mm; Dionex) with a flow rate of 1 ml·min<sup>-1</sup>. The column was pre-equilibrated in 0.25 M sodium acetate/0.10 M NaOH and FBP resolved by applying a 0.25–0.75 M linear gradient of sodium acetate (NaOH constant) developed 10–35 min after sample application. The column was regenerated with 0.90 M acetate/0.10 M NaOH, then made ready for the next sample by running under the initial conditions for 10 min.

CA was dehydrated from acidic solution to form the lactone, and then subjected to ion-moderated partitioning HPLC by using an Aminex HPX-87H (300 × 7.8 mm) organic acid column (Bio-Rad) with isocratic elution with 5 mM H<sub>2</sub>SO<sub>4</sub> at 0.4 ml·min<sup>-1</sup>. The CA-containing peak (at 14.3 min) was treated with a small excess of Dowex-1 (chloride form) to remove SO<sub>4</sub><sup>2-</sup>, followed by desiccation *in vacuo* over solid sodium hydroxide and anhydrous CaCl<sub>2</sub>. CA was finally resolved (retention time, 4.5 min) by anion-exchange HPLC with a CarboPac PA1 column (4 × 250 mm; Dionex) with isocratic elution by using 0.05 M sodium acetate/0.10 M NaOH at a flow rate of 1 ml·min<sup>-1</sup>. Because of the large amounts of hamamelose and CA in the transformed lines, final quantitation with the electrochemical detector required sample dilutions typically of 100-fold, before HPLC, to avoid detector saturation.

**Pulse-Chase Experiment.** A Perspex chamber was constructed to accommodate five leaf segments simultaneously (Fig. 2). The internal dimensions of the chamber (0.48 × 20.2 × 4.4 cm) gave an internal volume of 42.7 cm<sup>3</sup>. A gas inlet and outlet were provided at either end, and gas was delivered and collected through a perforated vertical spacer, which promoted uniform gas distribution within the chamber. The end incorporating the gas outlet could be removed, enabling sample access. Attached leaves were cut under water by using a rectangular, cushioned template (3.45 × 3.7 cm) with the central vein in the middle, running parallel to the long axis of the segment. The cut edge nearest the leaf base was placed in a water-filled polythene trough (capacity, 0.5–1.0 ml), water was removed from leaf surfaces by gentle blotting, and the segment with its trough was mounted in a holder (constructed from 0.013-mm-gauge brass sheet) that incorporated 6-cm<sup>2</sup> apertures (2.6 × 2.3 cm) on both faces (Fig. 2). Each holder incorporated a neodymium magnet (1.5 × 6 mm diameter; A1 Magnetics Ltd., Walkern, Hertfordshire, U.K.) to facilitate loading and removal from the chamber. The chamber was positioned parallel to a fluorescent strip light, which provided uniform illumination of 100 ± 5  $\mu\text{mol}\cdot\text{m}^{-2}\cdot\text{s}^{-1}$  to the upper leaf surface, at a constant temperature of 25 ± 1°C.

Air containing 1 mmol/mol (0.1% by volume) <sup>14</sup>CO<sub>2</sub> was generated by passing 2 liters of CO<sub>2</sub>-free air through 2.42 ml of 34.5 mM NaH<sup>14</sup>CO<sub>3</sub> (58 mCi·mmol<sup>-1</sup>) immediately after addition to 2 ml of 1 M H<sub>2</sub>SO<sub>4</sub>. The gas was dried by passage through anhydrous magnesium perchlorate and stored in a sealed, dou-

ble-walled polythene bag. Air containing 1 mmol/mol nonradiolabeled CO<sub>2</sub> was generated by combining 2.4 liters of 1% CO<sub>2</sub> in nitrogen with 21.6 liters of CO<sub>2</sub>-free, dry air in another sealed, double-walled polythene bag. Air was pumped through the leaf chamber by using a diaphragm pump (Charles Austin Ltd., Byfleet, U.K.) at the required flow rate, measured by a calibrated flow meter (Rotameter Manufacturing, Croydon, U.K.). The flow rate was set to limit depletion of CO<sub>2</sub> to ≤20% (100 cm<sup>3</sup>·min<sup>-1</sup> except for the first 60 s of the <sup>14</sup>CO<sub>2</sub> feed and the cold-chase, which were both at 150 cm<sup>3</sup>·min<sup>-1</sup>). Air containing 1 mmol CO<sub>2</sub>/mol (with or without radiolabel) was used throughout. As soon as the chamber contained five mounted leaf segments, photosynthetic induction was started. Air containing unlabeled CO<sub>2</sub> was pumped into the illuminated chamber for 12.5 min, during which a steady rate of photosynthesis was established. For the next 5 min, air containing <sup>14</sup>CO<sub>2</sub> was used (“pulse”), followed by unlabeled CO<sub>2</sub> (“chase”). Holders were removed from the chamber at the stated times by magnetic repulsion to fall directly into liquid nitrogen. This process took ≤1 s. To assess reproducibility, a mounted leaf that had been induced and exposed to <sup>14</sup>CO<sub>2</sub> for 5 min was included in every batch of five mounted leaf segments within the chamber (Fig. 7).

**Analysis of Samples from Pulse–Chase.** Frozen leaf material was extracted in acid and prepared for initial fractionation by using Dowex-1, as described above, except that a 0–1.0 M linear gradient of sodium formate (total volume, 25 ml) was applied. This approach allowed the resolution of neutrals, organic acids, monophosphates, and (CA1P + diphosphates) into four separate fractions. These fractions were passed through columns containing a 2-fold excess of Dowex-50 (H<sup>+</sup> form). After desiccation *in vacuo*, as above, the mono- and bisphosphate fractions were rehydrated (1 ml), the pH adjusted to 8.0 (NaOH), and mixed with 50 μl of a solution containing 10 units of alkaline phosphatase (Sigma P6772)/0.5 M Tris·HCl (pH 8.3)/10 mM MgCl<sub>2</sub>/0.1 mM ZnSO<sub>4</sub>. After 60 min at 25°C, the solution was vortexed with 100 μl of Dowex-1 (formate), recovered, then vortexed with 100 μl of Dowex-50 (H<sup>+</sup>), after which the supernatant was desiccated *in vacuo*, as before. In the following HPLC analyses, all samples were rehydrated in 300 μl, of which 100 μl was loaded per run. CA was purified from the organic acid fraction as already described. Hamamelose from the neutral fraction (or liberated from the mono- and bisphosphate fractions) was determined after purification (*i*) by ion-moderated partitioning HPLC, with an Aminex HPX-87H column (21) with Dowex-1 (Cl<sup>-</sup> form) removal of SO<sub>4</sub><sup>2-</sup> from the retained fractions; and (*ii*) by anion-exchange HPLC with a Dionex CarboPac MA1 (4 × 250 mm) column with isocratic elution with 0.48 M NaOH, a flow rate of 0.4 ml·min<sup>-1</sup>, and a run duration of 60 min per sample (Fig. 6). Fractions were collected at 0.5-min intervals in the vicinity of the peaks of interest, and the <sup>14</sup>C content of the purified components was determined by liquid scintillation spectrometry.

**Other Materials.** Radiolabeled and nonradiolabeled CA and CA1P were synthesized as described (10) from ribulose 1,5-bisphosphate and either potassium [<sup>14</sup>C]cyanide or nonradiolabeled potassium cyanide. Hamamelose was synthesized from D-fructose or [U-<sup>14</sup>C] D-fructose as described (23), and the chemical identity confirmed by <sup>13</sup>C NMR spectroscopy (24). [U-<sup>14</sup>C]FBP was synthesized enzymatically from D-[U-<sup>14</sup>C]fructose by using purified hexokinase, fructose-6-phosphate kinase, and ATP. Dowex resins (AG 50W-X8 and AG 1-X8) were supplied by Bio-Rad. Radiochemicals were supplied by Amersham Pharmacia.

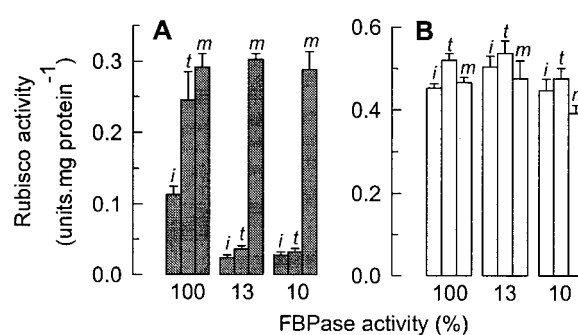


**Fig. 3.** Rubisco activity in leaves with different FBPase activities, in light and darkness. Freeze-clamped leaf discs from plants expressing 10%, 13%, or normal (100%) levels of FBPase activity were used to determine the activation state of Rubisco before dawn (filled bars) (A), or at midday (open bars, B; *i*, *t*, and *m*, as defined in the text). The stated carboxylase activity of Rubisco (CO<sub>2</sub> uptake) represents the mean ± SD from three independent determinations.

### Results

The possibility that CA1P was more abundant in potato leaves with reduced expression of FBPase was first investigated by assaying the accompanying carboxylase activity of Rubisco, after rapid extraction from leaves (Fig. 3). Comparison of the activity of Rubisco from the control with that from two extreme transformed lines, expressing 10% and 13% of the wild-type FBPase activity (Fig. 3A), showed that the (initial, *i*) activity of Rubisco at the time of extraction from leaves harvested before dawn, was 4- to 5-fold lower in the transformed lines. When measures were taken to activate any vacant, inactive catalytic sites by incubating the extracts with activating cofactors CO<sub>2</sub> and Mg<sup>2+</sup>, the resulting (total, *t*) activity was only significantly increased in the control. Only when measures were taken to remove tightly bound inhibitors from Rubisco in the extracts of the transformed lines was the activity of Rubisco increased to levels comparable with the control (maximal, *m*). Similar measurements with extracts from leaves harvested in the middle of the photoperiod showed that the initial, total, and maximal activities of all the extracts were high (Fig. 3B). Together, these experiments demonstrate a large increase in a nocturnal Rubisco inhibitor in the transformed plants.

Furthermore, the amounts of the CA1P precursors hamamelose (H) and CA in the antisense plants were dramatically increased (Fig. 4A), in particular, in the light (open bars) but also

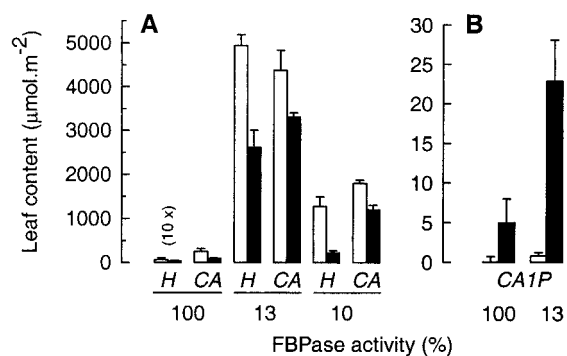


**Fig. 4.** Hamamelose, CA, and CA1P content of leaves with different FBPase activities, in light and darkness. Freeze-clamped leaf discs from plants expressing 10%, 13%, or normal (100%) levels of FBPase activity were used to determine the hamamelose (H) and CA content (A) and the CA1P content (B) at midday (open bars) or before dawn (filled bars). The hamamelose content of the control has been magnified 10-fold. Data represent the mean ± SD from three independent determinations.



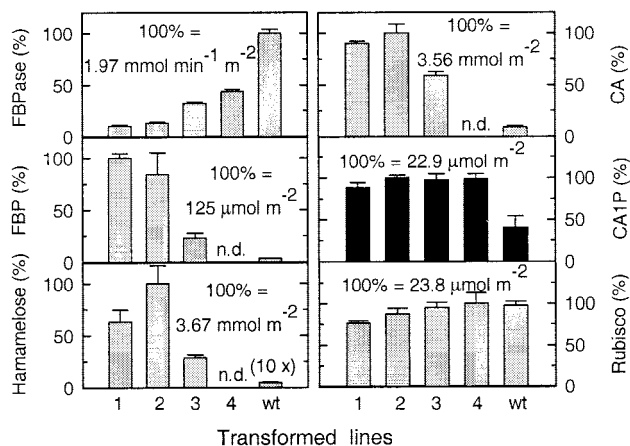


**Fig. 5.** Correlation between FBPAse activity, FBP, hamamelose, CA, CA1P, and Rubisco catalytic sites in control and antisense plants. Amounts are expressed as a percentage of the highest value within each group. Transformed lines possessed 10% (1), 13% (2), 32% (3), and 44% (4) of the FBPAse activity of the control (wt). Gray bars, light-sampled leaves; black bars, dark-sampled leaves. FBP, hamamelose, and CA were not determined (n.d.) for transformed line 4. Data represent the mean  $\pm$  SD from three independent determinations.

in the dark (filled bars) compared with the control. In light-adapted leaves of the 13% line, the amounts of hamamelose and CA exceeded those in the control by 780- and 17-fold, respectively. Under these conditions, hamamelose accounted for more carbon in the 13% line than sucrose and was as plentiful as sucrose in the wild type (the latter being  $5.1 \pm 0.6$  ( $n = 4$ ) mmol hexose equivalents  $m^{-2}$ ) (17). The amount of hamamelose in both transformed lines fell markedly in a subsequent period of darkness (Fig. 4A) indicating translocation or further metabolism. The extent of this decline ( $1\text{--}2$  mmol  $m^{-2}$ ) far exceeded the extent of CA1P biosynthesis ( $20\text{--}25$   $\mu\text{mol} \cdot m^{-2}$ , see below).

In support of the foregoing evidence (Fig. 3A and B) for elevated CA1P in the antisense plants in the dark, direct measurement of CA1P showed that the transformed plants indeed contained significantly more (in this case 4-fold) than the control (Fig. 4B).

Comparison of the FBPAse activity in a range of transformed lines (Fig. 5) with the corresponding amounts of the putative intermediates (FBP, hamamelose, and CA, all measured in the same leaf sample) and CA1P (sampled in a subsequent period of darkness) revealed that, although amounts of the proposed intermediates varied in proportion to the amount of FBP, the abundance of CA1P was increased to almost identical amounts across a range of transformed lines, with a mean value of  $21.9 \pm 1.2$   $\mu\text{mol} \cdot m^{-2}$ . It has already been demonstrated that the amount of Rubisco in control and transformed lines is similar (18). In the current work this was found to be  $21.7 \pm 2.3$   $\mu\text{mol}$  Rubisco catalytic sites  $m^{-2}$ , very similar to the amounts of CA1P in the transformed lines (mean values from Fig. 5).

The rate at which  $^{14}\text{C}$  passed through the proposed intermediates during steady-state photosynthesis after a 5-min exposure to  $^{14}\text{CO}_2$  was examined. Leaf segments from French bean were used, as described under *Materials and Methods*. The whole process was conducted with  $\text{CO}_2$  at approximately three times the atmospheric concentration, both to suppress the passage of  $^{14}\text{C}$  into photorespiratory intermediates and to maximize the incorporation of radiolabel into the putative intermediates during the brief period of photosynthesis at low irradiance. Such low irradiance ( $100$   $\mu\text{mol} \cdot m^{-2} \cdot s^{-1}$ ) favors the incorporation of  $^{14}\text{C}$  into CA1P (20). After 5 min of exposure, about  $36$   $\mu\text{Ci}$  of  $^{14}\text{C}$  had become incorporated into acid-stable, soluble products within a

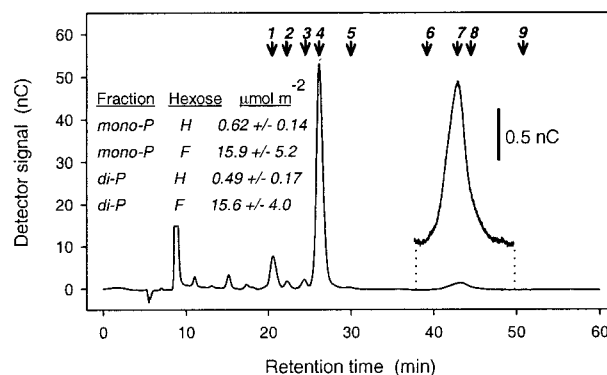


**Fig. 6.** Elution profile of sugars derived from a monophosphate fraction, after anion-exchange HPLC (CarboPac MA1 analytical column). The corresponding profile for the bisphosphate fraction was very similar. Numbered arrows show peak retention times of mannose (1), glucose (2), galactose (3), fructose (4), ribose (5), hamamelitol (6), hamamelose (7), sucrose (8), and sedoheptulose (9). The hamamelose peak is also shown after expansion of the ordinate axis. (Inset) The amounts of hamamelose (H) and fructose (F) determined by this procedure in the mono- and bisphosphate fractions of French bean leaves, 5 h into the photoperiod, being the mean and SD of four independent determinations.

leaf segment, which declined by a factor of 3 during the chase period, presumably because of respiration, to approximately  $13$   $\mu\text{Ci}$ , 115 min later. Integral to this study was the resolution of HBP and HMP from the extracted metabolites. Thus, the mono- and bisphosphate fractions were resolved (by Dowex-1 chromatography) and the parent sugars released by treatment with alkaline phosphatase. Subsequent purification of hamamelose was achieved by two successive HPLC procedures, the final step being anion exchange at high pH (Fig. 6). In this way, HMP and HBP were estimated to be present at concentrations of  $0.62 \pm 0.14$  and  $0.49 \pm 0.17$   $\mu\text{mol} \cdot m^{-2}$ , respectively. Chemically synthesized HMP and HBP were not available, so the recovery could not be assessed directly. However, parallel identification of fructose liberated from extracted fructose mono- and bisphosphates (Fig. 6 Inset) yielded values of  $15.9 \pm 5.2$  and  $15.6 \pm 4.0$ , approximately 50% of the values in French bean determined by Badger *et al.* (25). The retention times of a variety of other sugars were also characterized by using the same HPLC procedure (Fig. 6). Contamination with sucrose (derived from the monophosphate fraction as sucrose 6-phosphate), whose retention time was close to that of hamamelose, was avoided by the initial HPLC step, which gave baseline resolution of both components (21). Erythrose, xylulose, glyceraldehyde, and ribulose (or breakdown products thereof) were barely detectable and did not overlap with either hamamelose or fructose (not shown). Complementing the vastly elevated amounts of free hamamelose and carboxyarabinitol found in potato plants expressing 13% of the control FBPAse activity, such plants were also found to contain  $14.4 \pm 6.5$  and  $7.6 \pm 1.1$   $\mu\text{mol} \cdot m^{-2}$  of HMP and HBP, respectively ( $n = 2$ ), in the light, whereas the amounts in the control plants were below the limits of detection ( $<0.1$   $\mu\text{mol} \cdot m^{-2}$ ).

The pattern of  $^{14}\text{C}$  entry into and exit from FBP, HBP, HMP, H, and CA revealed a definite progression (Fig. 7A and B). FBP and HBP were the first to be maximally labeled, after a 5-min pulse of  $^{14}\text{CO}_2$ , after which the FBP was quickly metabolized, as evidenced by the rapid decline of  $^{14}\text{C}$  after the onset of the cold-chase (Fig. 7A,  $\bullet$ ). The amount of [ $^{14}\text{C}$ ]HBP remained fairly constant during the 5-min period from the removal of  $^{14}\text{CO}_2$ , but then declined to 30% of this level during the next 5 min (Fig. 7A,  $\blacktriangledown$ ). Here, as with subsequent metabolites, the slower incorporation of  $^{14}\text{C}$  was consistent with HBP being formed after FBP, whereas the slower subsequent decline of

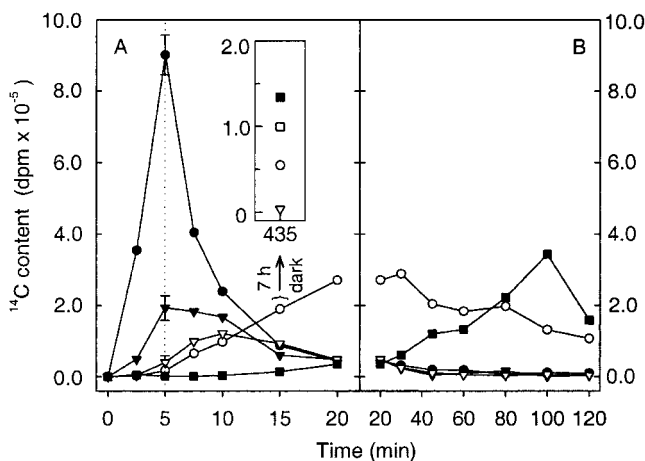


**Fig. 7.**  $^{14}\text{C}$  content of putative intermediates of CA1P biosynthesis as a function of time, during and after exposure to  $^{14}\text{CO}_2$ . After photosynthetic induction, leaf segments were exposed to 0.1%  $^{14}\text{CO}_2$  for 5 min, followed by 0.1%  $^{12}\text{CO}_2$  (transition indicated by vertical dotted line). At the indicated times samples were removed and immediately frozen in liquid N. The presence of specific  $^{14}\text{C}$ -labeled metabolites was determined: ●, FBP; ▼, HBP; ▽, HMP; ○, hamamelose; and ■, CA. The data are divided into two parts (A and B) depending on the duration of the cold-chase. Assays at 5 min show the mean ( $\pm$ SD) of three independent samples (errors within boundaries of symbols not shown). An additional sample (*Inset*) was removed from the chamber after 15 min and kept in darkness in normal air for 7 h before freezing. The CA1P content ( $\square$ ) of this sample was also determined, after affinity purification and HPLC (20).

$^{14}\text{C}$ ]HBP was consistent both with the continuing supply of  $^{14}\text{C}$  from FBP and with the slower subsequent utilization of this metabolite. The maximal incorporation of  $^{14}\text{C}$  into HMP occurred later than that into HBP (Fig. 7A, ▽). Hamamelose became maximally labeled 25 min into the cold chase (Fig. 7A and B, ○). No  $^{14}\text{C}$ ]hamamelose was evident before the incorporation of  $^{14}\text{C}$  into the hamamelose phosphates, and no more  $^{14}\text{C}$ ]hamamelose was formed after the  $^{14}\text{C}$  in the hamamelose phosphates had been depleted (Fig. 7B). Similarly, the first appearance of  $^{14}\text{C}$  in CA (at 15 min in Fig. 7A, ■) followed the appearance of considerable quantities of  $^{14}\text{C}$  in hamamelose, and the subsequent gradual increase in  $^{14}\text{C}$ ]CA mirrored a parallel decline in  $^{14}\text{C}$ ]hamamelose. The decline in  $^{14}\text{C}$ ]CA at 120 min suggested that it was also being metabolized. The passage of  $^{14}\text{C}$  from  $\text{CO}_2$  into these compounds occurred in the light. However, significant incorporation of  $^{14}\text{C}$  from recently assimilated carbon into CA1P requires a subsequent period of darkness (20). Thus, 15 min after photosynthetic induction a leaf segment was removed from the chamber and kept in darkness for 7 h, after which it was rapidly frozen in liquid nitrogen. The corresponding amounts of  $^{14}\text{C}$  detected in CA and CA1P were 134,000 dpm (■) and 99,000 dpm ( $\square$ ) per leaf segment, respectively (Fig. 7A *Inset*).

## Discussion

The foregoing results are consistent with the proposal that FBP is the link between primary carbon assimilation and the *de novo* synthesis of CA1P (13, 16). We have shown that the flow of  $^{14}\text{C}$  from  $\text{CO}_2$  to CA in the light (Fig. 7) is entirely consistent with previous investigations relating  $\text{CO}_2$  to HBP (15), FBP to hamamelose (14), and hamamelose to CA (16). The precursor-product relationship between CA and CA1P has already been established (17) and confirmed (16, 22), whereas the transfer of  $^{14}\text{C}$  from photoassimilate into CA1P (20) under the present conditions is demonstrated in Fig. 7. In addition, the increase in hamamelose, CA, and CA1P accompanying an increase in FBP

(Figs. 4 and 5) strongly endorses the proposed pathway for CA1P biosynthesis (Fig. 1). The dephosphorylation of HBP, oxidation of hamamelose to CA, followed by rephosphorylation yielding CA1P seems elaborate, but (a) it may be necessary to avoid the synthesis of carboxyarabinitol-1,5-bisphosphate (a virtually irreversible inhibitor of Rubisco (26) that would result from the direct oxidation of HBP); and (b) may reflect the evolution of CA1P biosynthesis from a preexisting metabolic pathway involving hamamelose (see below).

Details relating to the conversion of FBP into HBP have already been elucidated by Beck and coworkers. As reviewed by Grisebach (27) the fate of glucose labeled either with  $^{14}\text{C}$  at specific positions (28) or with  $^3\text{H}$  attached to specific carbon atoms (14) all strongly indicate a reaction mechanism involving the direct conversion of FBP into HBP without the involvement of free 3-carbon intermediates, such as triose phosphates. The conversion of FBP into HBP by isolated chloroplast material demonstrated by Glick and Beck (14) might be challenged on the grounds of cytosolic contamination. However, in view of the very rapid saturation of HBP with  $^{14}\text{C}$  after photoassimilation of  $^{14}\text{CO}_2$  by whole leaves, which was comparable with the rate of saturation of Calvin cycle intermediates; the absolute light dependence of  $^{14}\text{C}$  incorporation into HMP; and the likely rearrangement of the carbon skeleton accompanying HBP synthesis (14, 28), little doubt exists that this reaction was catalyzed by chloroplast enzyme(s). Even if the conversion had been catalyzed by contaminating cytosolic enzymes, the fact remains that leaf extracts promoted the conversion of FBP into HBP.

The amount of FBP in photosynthesizing leaves can be greater during periods of low irradiance ( $<100 \mu\text{mol photons m}^{-2}\text{s}^{-1}$ ) than at higher irradiances (29). Carbon assimilated during similarly low irradiance has been most readily incorporated into CA and CA1P (20). The proposed precursor-product relationship between FBP and CA1P can account for these observations in terms of FBP abundance. The rate of incorporation of  $^{14}\text{C}$  from  $^{14}\text{CO}_2$  into intermediates up to and including hamamelose has been shown to be rapid;  $^{14}\text{C}$  appears in hamamelose after 2.5 min (14) or 5 min (Fig. 7A) of exposure to  $^{14}\text{CO}_2$ . Therefore the distinct lag in the incorporation of  $^{14}\text{C}$  from  $^{14}\text{CO}_2$  into CA1P demonstrated (20) may be due to dilution of radiolabel in pools of preexisting (unlabeled) hamamelose and/or CA, making the onset of incorporation into CA1P more difficult to detect. Alternatively, steps toward the biosynthesis of CA1P may not be exclusively localized in the chloroplast, resulting in a delay if the passage of the relevant intermediates between subcellular compartments was slow. Indeed, chloroplast-uptake experiments have shown that hamamelose passes across the chloroplast envelope at the same rate as glucose, whereas CA is an order of magnitude slower (M.A.J.P., P.J.A., and J. C. Servaites, data not shown). Fig. 7B shows a short delay in the appearance of  $^{14}\text{C}$ ]CA, which was detected from as little as 15 min into the feeding experiment. However, the relatively slow appearance of label as CA1P (20) could be due to the slow entry of  $^{14}\text{C}$ ]CA into the chloroplast from a cytosolic site of synthesis.

Indeed, although CA1P is located exclusively in the chloroplast (30, 31), and even though kinetic and chloroplast feeding experiments of Glick and Beck (14) provide strong evidence that the synthesis of HBP takes place in the chloroplast, it is not known whether every step in the synthesis of CA1P takes place in the chloroplast. For example, CA is not restricted to the chloroplast and its intracellular distribution is light-dependent (19). Whereas the relatively low CA content of chloroplasts from dark-adapted leaves is likely to result from net phosphorylation (to CA1P) and export (from the chloroplast) following the transition from light to dark, the fluctuations of CA in other compartments (19) may be due not only to redistribution but also to CA synthesis outside the chloroplast.

Preliminary experiments indicated a larger flux of  $^{14}\text{C}$  from  $\text{CO}_2$  to CA1P in leaves of French bean than of potato and conditions promoting this pathway in French bean had already been established (20). Therefore, French bean was chosen for the pulse–chase experiment (Fig. 7). Although 13% FBPase plants contained more HBP and HMP than French bean, the amounts of hamamelose and CA in these leaves (Fig. 4A) were very high, even after a prolonged period of darkness. Such preexisting pools of precursors may cause considerable dilution of radiolabel from recently assimilated  $^{14}\text{C}$  and for this reason the transgenic potato was considered unsuitable. Indeed, in pilot pulse–chase experiments with potato,  $^{14}\text{C}$  labeled CA1P was detected in wild type but not 13% FBPase leaves (not shown).

The large increases in abundance of the precursors hamamelose and CA contrast with the relatively modest increases in CA1P in the transformed lines (Figs. 4 and 5). The almost equal amounts of CA1P and Rubisco catalytic sites in the transformed lines (Fig. 5) suggest that the upper limit on CA1P concentration may be determined by the concentration of Rubisco catalytic sites rather than the abundance of its immediate precursors. In this case, it would be likely that excess, unbound CA1P was dephosphorylated by the CA1P-specific phosphatase (8–10). On the basis of measurement of predawn and midday Rubisco activities, few species contain sufficient CA1P to occupy every available Rubisco catalytic site (32–35), and only in *P. vulgaris* have dark adapted leaves been found to contain more CA1P than Rubisco active sites (36, 37). Because the accumulation of CA1P is governed in principle by the relative rates of synthesis, degradation and its interaction with Rubisco, the balance between these factors evidently differs between species.

The accumulation of hamamelose and CA in plants with reduced FBPase activity, the time-dependent passage of  $^{14}\text{C}$  through the proposed intermediates, and the conversion of these intermediates into CA1P during leaf-feeding experiments with chemically synthesized,  $^{14}\text{C}$ -labeled precursors reported elsewhere (16, 17); all support the proposed pathway of *de novo* synthesis of CA1P (Fig. 1). Although the existence of alternative pathways of CA1P biosynthesis cannot be ruled out, the existence of the proposed pathway is strongly supported by the present work.

Although many plant species (e.g., rice, soya, potato, tobacco, and tomato) synthesize sufficient CA1P to have a significant effect on Rubisco, others (e.g., wheat and maize) do not (32, 38), even though they contain CA (19). Knowledge of the pathway of CA1P biosynthesis will facilitate future studies into the function of CA1P in plants. One intriguing aspect of this work relates to the fate of hamamelose and CA in the transformed plants that were not used for CA1P synthesis (Fig. 4A). Although hamamelose is thought to be ubiquitous among higher plants (39), with involvement in compatible solute, disaccharide, and hydrolyzable tannin formation (40) in certain species, a ubiquitous role has yet to be established. Transgenic material containing vastly increased amounts of these branched-chain intermediates will be useful in identifying additional roles for these compounds and in further exploring the biosynthetic pathway.

We thank Dr. Tony Hooper for conducting NMR analyses and Mr. Andrew Pastor for translating German research papers. This work was supported by the Biotechnology and Biological Sciences Research Council of the United Kingdom. The Institute of Arable Crops Research receives grant-aided support from the Biotechnology and Biological Sciences Research Council.

- Parry, M. A. J., Loveland, J. R. & Andralojc, P. J. (1999) in *Plant Carbohydrate Biochemistry*, eds. Bryant, J., Burrell, M. & Kruger, N. (BIOS Scientific Publishers, Oxford), pp. 127–145.
- Cleland, W. W., Andrews, T. J., Gutteridge, S., Hartman, F. C. & Lorimer, G. H. (1998) *Chem. Rev.* **98**, 549–561.
- Gutteridge, S., Parry, M. A. J., Burton, S., Keys, A. J., Mudd, A., Feeney, J., Servaites, J. & Pierce, J. (1986) *Nature (London)* **324**, 274–276.
- Berry, J. A., Lorimer, G. H., Pierce, J., Seemann, J. R., Meek, J. & Freas, S. (1987) *Proc. Natl. Acad. Sci. USA* **84**, 734–738.
- Kobza, J. & Seemann, J. R. (1989) *Plant Physiol.* **89**, 918–924.
- Sage, R. F., Reid, C. D., Moore, B. D. & Seemann, J. R. (1993) *Planta* **191**, 222–230.
- Robinson, S. P. & Portis, A. R. (1988) *FEBS Lett.* **233**, 413–416.
- Holbrook, G. P., Bowes, G. & Salvucci, M. (1989) *Plant Physiol.* **90**, 673–678.
- Gutteridge, S. & Julien, B. (1989) *FEBS Lett.* **254**, 225–230.
- Kingston-Smith, A. H., Major, I., Parry, M. A. J. & Keys, A. J. (1992) *Biochem. J.* **287**, 821–825.
- Parry, M. A. J., Andralojc, P. J., Parmar, S., Keys, A. J., Habbash, D., Paul, M., Alred, R., Quick, W. P. & Servaites, J. C. (1997) *Plant Cell Environ.* **20**, 528–534.
- Khan, S., Andralojc, P. J., Lea, P. J. & Parry, M. A. J. (1999) *Eur. J. Biochem.* **266**, 840–847.
- Beck, E., Scheibe, R. & Reiner, J. (1989) *Plant Physiol.* **90**, 13–16.
- Gilck, H. & Beck, E. (1974) *Z. Pflanzenphysiol.* **72**, 395–409.
- Beck, E., Stransky, H. & Fürbringer, M. (1971) *FEBS Lett.* **13**, 229–234.
- Andralojc, P. J., Keys, A. J., Martindale, W., Dawson, G. W. & Parry, M. A. J. (1986) *J. Biol. Chem.* **271**, 26803–26809.
- Moore, B. D. & Seemann, J. R. (1992) *Plant Physiol.* **99**, 1551–1555.
- Kossmann, J., Sonnewald, U. & Willmitzer, L. (1994) *Plant J.* **6**, 637–650.
- Moore, B. D., Sharkey, T. D., Kobza, J. & Seemann, J. R. (1992) *Plant Physiol.* **99**, 1546–1550.
- Andralojc, P. J., Dawson, G. W., Parry, M. A. J. & Keys, A. J. (1994) *Biochem. J.* **304**, 781–786.
- Andralojc, P. J., Keys, A. J., Adam, A. & Parry, M. A. J. (1998) *J. Chromatogr. A* **814**, 105–110.
- Martindale, W., Parry, M. A. J., Andralojc, P. J. & Keys, A. J. (1997) *J. Exp. Bot.* **48**, 9–14.
- Yanagihara, R., Osani, S. & Yoshikawa, S. (1992) *Chem. Lett.* 89–90.
- Schilling, G. & Keller, A. (1977) *Liebigs Ann. Chem.* 1475–1479.
- Badger, M. R., Sharkey, T. D. & von Caemmerer, S. (1984) *Planta* **160**, 305–313.
- Pierce, J., Tolbert, N. E. & Barker, R. (1980) *Biochemistry* **19**, 934–942.
- Grisebach, H. (1980) in *The Biochemistry of Plants*, ed. Preiss, J. (Academic, New York), Vol. 3, pp. 171–197.
- Beck, E., Sellmair, J. & Kandler, O. (1968) *Z. Pflanzenphysiol.* **58**, 434–451.
- Sassenrath-Cole, G. F. & Percy, R. W. (1994) *Plant Physiol.* **105**, 1115–1123.
- Moore, B. D., Sharkey, T. D. & Seemann, J. R. (1995) *Photosynth. Res.* **45**, 219–224.
- Parry, M. A. J., Andralojc, P. J., Lowe, H. M. & Keys, A. J. (1999) *FEBS Lett.* **444**, 106–110.
- Servaites, J. C., Parry, M. A. J., Gutteridge, S. & Keys, A. J. (1986) *Plant Physiol.* **82**, 1161–1163.
- Seemann, J. R., Berry, J. A., Freas, S. M. & Krump, M. A. (1985) *Proc. Natl. Acad. Sci. USA* **82**, 8024–8028.
- Vu, J. C., Allen, L. H. & Bowes, G. (1984) *Plant Physiol.* **76**, 843–845.
- Holbrook, G. P., Turner, J. A. & Polans, N. O. (1992) *Photosynth. Res.* **32**, 37–44.
- Moore, B. D., Kobza, J. & Seemann, J. R. (1991) *Plant Physiol.* **96**, 208–213.
- Moore, B. D., Kiirats, O., Charlet, T. & Seemann, J. R. (1995) *Plant Cell Physiol.* **36**, 1097–1103.
- Vu, J. C. V., Allen, L. H., Boote, K. J. & Bowes, G. (1997) *Plant Cell Environ.* **20**, 68–76.
- Sellmair, J., Beck, E., Kandler, O. & Kress, A. (1977) *Phytochemistry* **16**, 1201–1204.
- Beck, E. (1982) in *Encyclopedia of Plant Physiology*, eds. Loewus, F. A. & Tanner, W. (Springer, Berlin), Vol. 13A, pp. 124–157.